Machine learning bridges microslips and slip avalanches of sheared granular gouge

Gang Ma[1,2], Jiangzhou Mei[1,2], Ke Gao[3], Jidong Zhao[4], Wei Zhou[1,2], Di Wang[1,2]

[1] State Key Laboratory of Water Resources and Hydropower Engineering Science, Wuhan University, Wuhan 430072, China.

[2] Key Laboratory of Rock Mechanics in Hydraulic Structural Engineering of Ministry of Education, Wuhan University, Wuhan 430072, China.

[3] Department of Earth and Space Sciences, Southern University of Science and Technology, Shenzhen 518055, Guangdong, China.

[4] Department of Civil and Environmental Engineering, The Hong Kong University of Science and Technology, Clear Water Bay, Kowloon, Hong Kong, China

Corresponding author: Jiangzhou Mei (whu_meijz@whu.edu.cn)

Key Points:

- The microslips of sheared granular gouge demonstrate different statistical and spatial characteristics in stick and slip states
- Clustering of large microslips is correlated closely to large stress drop
- Machine learning establish a quantitative relationship between microslips and global stress fluctuations

Abstract

Understanding the origin of stress avalanche of fault gouges may offer deeper insights into many geophysical processes such as earthquakes. Microslips of sheared granular gouges were found to be precursors of large slip events, but the documented relation between local and global avalanches remains largely qualitative. We examine the stick-slip behavior of a slowly sheared granular system using discete element method simulations. The microslips, i.e., local avalanche events, are found to demonstrate significantly different statistical and spatial characteristics between the stick and slip states. We further investigate the correlation between the global stress fluctuations and the features extracted from microslips based on the machine learning (ML) approach. The data-driven model that incorporates the information of the spatial distribution of microslips can robustly predict the magnitude of stress fluctuation. A further feature importance analysis confirms that the spatial patterns of microslips manifest key information governing the global stress fluctuations.

Plain Language Summary

Frictional instability of natural fault gouges may play a key role in numerous geophysical processes, such as earthquakes and debris flows. Direct investigation of natural faults is difficult owing to their burial depth and broad distribution beneath the earth. Structural and statistical similarities between granular materials and fault gouges render the former an ideal model system for understanding the mechanism of natural fault gouges. When slowly deformed, granular materials generate cycles of friction increase and reduction, i.e., stick-slip cycles, analogous to the earthquake cycles. Microslips are found to be precursors of large slip events, but their correlations are mostly qualitative. This study uses numerical simulations to generate a series of stick-slip cycles of slowly sheared granular gouge. Distinctive differences are observed in the statistical and spatial characteristics of microslips between stick and slip stages. A trained machine learning model is further used to predict the global slip avalanche from the features extracted from microslips and its prediction accuracy can be significantly improved when considering the spatial information of microslips. This work suggests that the microslips detected inside natural gouge faults (e.g., local acoustic emission signal or local seismic wave) and their locations can be used to assess their frictional stability.

1 Introduction

The frictional stability of fault gouge layers underpins key understandings to many geophysical processes, including but not limited to earthquakes, debris flows, and landslides (Song et al., 2017; Ren et al., 2019; Nanjo, 2020). A granular gouge subjected to slow shearing demonstrates a typical stick-slip behavior, which plays a crucial role in triggering the frictional stability of the fault (Byerlee & Brace, 1966; Marone et al., 1991; Aharonov & Sparks, 2004; Denisov et al., 2016; Dorostkar & Carmeliet, 2019). Therefore, the stick-slip behavior of sheared granular gouges has been studied extensively in both laboratory experiments (Marone, 1998; Niemeijer et al., 2010; Scuderi et al., 2015, 2016; Leeman et al., 2016; Tinti et al., 2016; Rivière et al., 2018) and numerical simulations (Aharonov & Sparks, 2004; Mair & Hazzard, 2007; Ferdowsi et al., 2014b; Dorostkar et al., 2017a; Gao et al., 2018; Ma et al., 2020). Particular attention has been placed on the influences of controlling factors on the stick-slip dynamics of granular gouge, such

as the wall geometry and friction (Rathbun et al., 2013), presence of liquids (Dorostkar et al., 2017b, 2018), particle characteristics (Mair et al., 2002; Dorostkar & Carmeliet, 2019), boundary vibration (Ferdowsi et al., 2014a), normal pressure (Gao et al., 2018), particle size polydispersity (Ma et al., 2020), and particle breakage (Wang et al., 2020). These studies offer novel insights into the complex dynamic behaviors of natural fault gouges and earthquake physics.

However, the microscopic origin of slip avalanche of slowly deformed granular gouge remains poorly understood. To address this issue, Johnson et al. (2013) employed a biaxial shear apparatus to investigate the physics of laboratory earthquake and found that the acoustic emission and microslip exhibit an exponential increase in the rate of occurrence, reaching a peak at the onset of slip avalanche. The corresponding DEM simulations comfirmed that the microslip event rate correlates well with large slip event onset (Ferdowsi et al., 2013). Microslip or local avalanche is essentially a result of the localized particle rearrangements (Ma et al., 2021). Due to the disordered structure of granular materials, a microslip may trigger nearby microslips, and the accumulation of these microslips may give rise to a global stress avalanche (Castellanos & Zaiser, 2018; Cao et al., 2019). Thus, microslips are widely regarded as precursors of large slip events and can be used to predict frictional weakening (Bolton et al., 2019, 2020; Trugman et al., 2020).

Furthermore, the statistics of local and global avalanches reveal a simple relation between the number of local avalanches and the global avalanches (Barés et al., 2017). The spatial characteristics of microslips are also closely correlated with the stress avalanche, where large stress drop is accompanied by a series of connected localized zones spanning the entire system, whereas during the elastic regime, the microslip events occur with low concentration and are spatially dispersed (Cao et al., 2018). Other particle scale metrics, such as coordination number, sliding contact ratio, potential energy, kinetic energy, evolves correspondingly during the stick phase and slip instability (Ferdowsi et al., 2015; Barés et al., 2017; Dorostkar & Carmeliet, 2018; Ma et al., 2020). Thus, studying the microscopic structure and dynamics of a granular gouge may help to unveil its stick-slip behaviors (Cipelletti et al., 2019).

Unfortunately, existing findings on the relation between microslips and global stress avalanche remains largely qualitative, whereas further advance on the subject matter demands quantitative correlations to be established. In this letter, we employ the machine learning (ML) approach to bridge the microslips and global stress fluctuations, including both stress recharge (stick regime) and stress drop (slip regime). ML offers data-driven approaches to automatically investigate the underlying relations between variables and facilitate the process of revealing complex and inexplicit patterns of large datasets (Marone, 2018; Bergen et al., 2019; Ren et al., 2020). Particularly, ML has gained increasing popularity in recent years and has been widely used in many areas of geoscience, such as predicting the timing and size of laboratory earthquakes (Rouet-Leduc et al., 2017; Corbi et al., 2019), revealing the frictional state of granular fault (Rouet-Leduc et al., 2018; Ren et al., 2019), estimating earthquake magnitude and GPS displacement rate (Rouet-Leduc et al., 2019; Mousavi & Beroza, 2020), and performing earthquake early warning and earthquake detection (Rouet-Leduc et al., 2018; Hulbert et al., 2019; Mousavi et al., 2020; Trugman et al., 2020).

To do so, we perform the discrete element method (DEM) simulations of quasi-static shear of granular gouge to achieve stick-slip dynamics. The microslip is manifested as the particle rearrangements and quantified by the nonaffine particle motion. Then we compare between the statistical and spatial characteristics of microslips in the stick and slip regimes. We use a two-step scheme for feature selection to consider both the statistical and spatial characteristics of microslips in the ML model training. The trained XGBoost model can well predict the global stress fluctuation from the features extracted from the microslips. Finally, we analyze the feature importance of the trained ML model and conclude that the spatial patterns of microslips contain key information about the stick-slip dynamics of granular gouge.

2 Materials and Methods

DEM simulations of simple shear tests were performed to obtained data of microslips and global stress fluctuations during the stick-slip cycles of granular gouge. Figure 1a shows the simple shear model setup of the granular gouge, which consists of 9,134 particles with diameters uniformly distributed from $0.8\,d_{50}$ to $1.2\,d_{50}$, where the average particle diameter d_{50} =1.25 mm. The size of the granular gouge sample is $32\,d_{50}$ (length) × $16\,d_{50}$ (depth) × $16\,d_{50}$ (height). The granular gouge is confined by two rough particle walls used to apply the shear loading and normal pressure. The top wall is fixed in the shear direction, while the normal pressure is maintained constant by a servo-control at 10 MPa. The granular gouge is sheared by moving the bottom wall in the x direction with a constant velocity while the vertical movement is constrained. The shear rate $\dot{\gamma}$, defined as the ratio of shear velocity to the undeformed sample height, is set to 0.05 to achieve stick-slip dynamics.

The numerical simulation is performed by the DEM code LIGGGHTS (Kloss et al., 2012). The Hertz-Mindlin contact model with Coulomb sliding friction is employed to simulate the contacts and deformation between particles. The particles have a density of 2900 kg/m^3, a Poisson's ratio of 0.25, Young's modulus of 65 GPa, a friction coefficient of 0.1, and a restitution coefficient of 0.87 (Ma et al., 2020). The wall particles adopt the same material properties as those in the shear body. The friction coefficient between the particle walls and the shear body is set to 0.9 to enhance surface friction. To collect enough data for the subsequent machine learning, we shear the granular gouge up to a shear strain of 50%. The evolution of normalized shear stress, defined as the ratio of shear stress σ to the applied normal pressure p, is shown in Figure 1b. When it is sheared into the steady-state regime, the gouge is found to undergo typical intermittent dynamics and serrated plastic flow. This phenomenon is seen to be universal in many amorphous solids like metal glasses (Sun et al., 2012; Cao et al., 2018), and porous materials (Baró et al., 2013).

The enlarged view of the dotted box shown in Figure 1b demonstrates that each stick-slip cycle starts with a nonlinear recharge of shear stress and is followed by a rapid drop. The recharge and drop of shear stress correspond to the stick and slip stages, respectively. We define stress fluctuation as the change of shear stress at the start and end of the recharge/drop events. Thus, the stress fluctuation of a drop event is positive, and the recharge event negative. Only the

magnitude of stress fluctuation greater than a threshold of 10^{-5} is considered. During the slow shearing of granular gouge, we recorded 3,191 stress drop and recharge cycles.

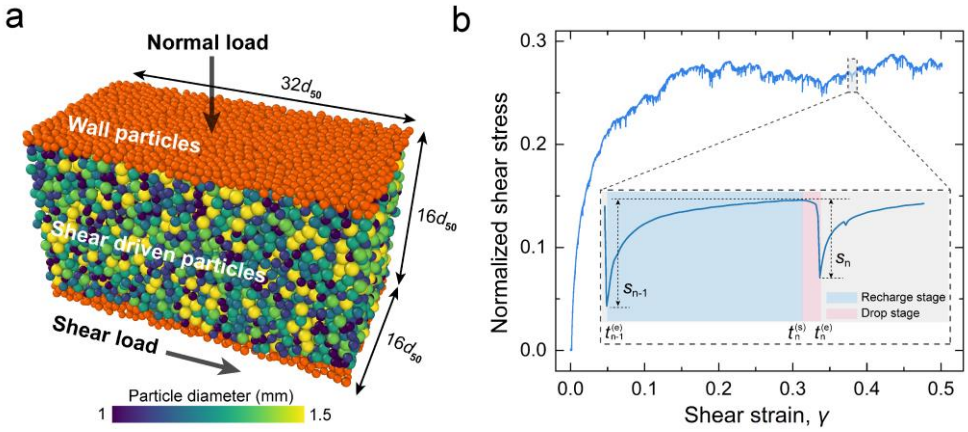

Figure 1. (a) Setup of the DEM experiment. Normal pressure and shear displacement are respectively applied on the top and bottom particle walls. Periodic boundary conditions are applied in the shear and depth directions. (b) Stress-strain curve resulted from the DEM simulation. The *y* axis denotes the shear stress σ normalized by the normal pressure p. The inset shows the enlarged stick-slip cycle which consists of stress recharge and drop stage represented by the blue and red shaded region, respectively.

3 Results

3.1 Statistical and spatial characteristics of microslips

The microslips that occurred during the recharge and drop events are manifested as irreversible particle rearrangements which are hereby quantified by the nonaffine particle displacements $D^2_{\min}$ (see Text S1) (Ma et al., 2021). It should be noted that many other quantities, such as local displacement, local energy fluctuation (Barés et al., 2017; Zheng et al., 2018), granular temperature (Ma et al., 2018, 2019), local acoustic emission (Trugman et al., 2020), force chain bulking (Gao et al., 2019; Liu et al., 2020) can also be used for characterizing microslips. Figure 2a and 2b show the spatial distributions of $D^2_{\min}$ during the recharge stage and the drop stage of a typical stick-slip cycle. Particles with higher $D^2_{\min}$ are colored in red. Due to the discrete nature and corporative particle motion of granular materials, the deformation of granular gouge occurs as a succession of localized micro-slips distributed within the system. Intuitively, the microslips are scattered throughout the granular gouge during the recharge stage. During the drop stage, the microslips are more spatially concentrated and tend to establish large stress avalanches inside the granular gouge.

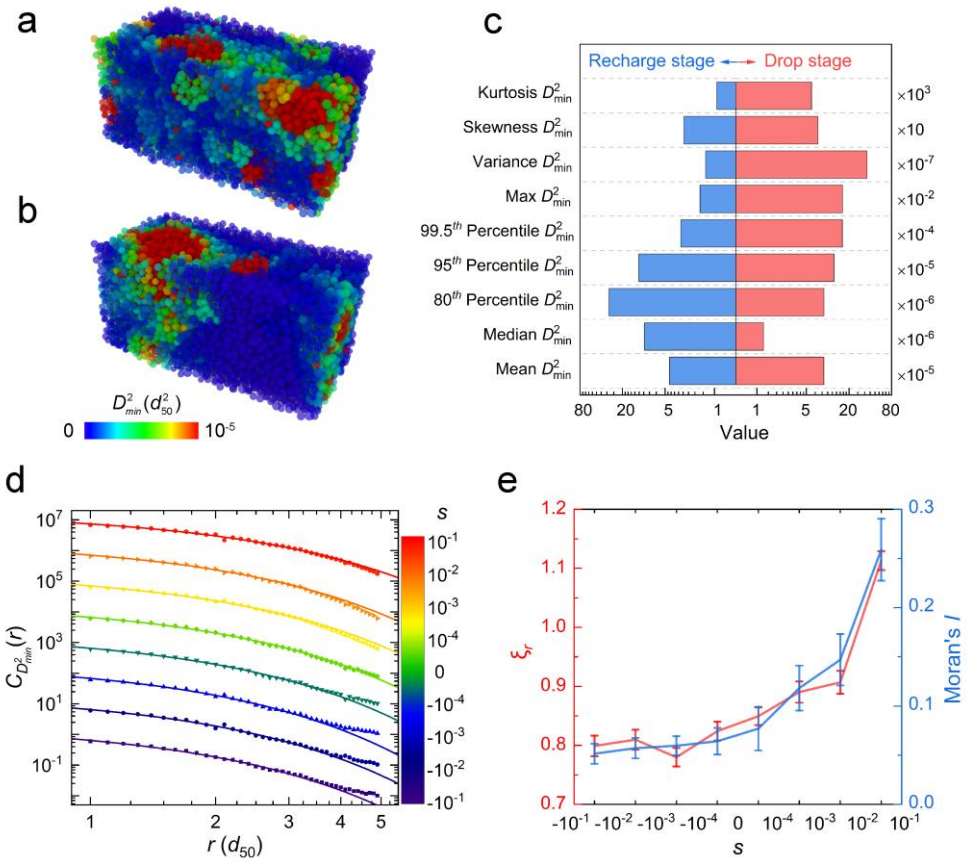

Figure 2. Statistical and spatial characteristics of microslips occurred during recharge and drop stages. Spatial maps of $D^2_{\min}$ occurred during the (a) recharge state and (b) drop stage of a typical stick-slip cycle. (c) Comparison of the statistical quantities of $D^2_{\min}$ during the recharge and drop stage. (d) Normalized spatial correlation function of $D^2_{\min}$ between two particles separated by distance r where r is in unit of the mean particle diameter. The data points are averaged over the recharge or drop stages falling into each bin. Solid lines are fits to the Ornstein-Zernike function. The data points and fitting lines of the different bin are shifted vertically for better visualization. (e) Evolutions of correlation length ξ_r and Moran' I with the magnitude of stress fluctuation. The error bar represents the standard deviation. Note that (d) and (e) are calculated over all stick-slip cycles.

Figure 2c compares the statistical features of microslips that occurred during the recharge stage (blue) and drop stage (red) of a stick-slip cycle. The microslips demonstrate significantly different statistical characteristics at the recharge stage and drop stage. For example, the 99.5^{th} percentile, max, variance, skewness, and kurtosis are larger for drop stage. The difference in statistics of microslips may suggest different underlying mechanism for stress recharge and stress drop. The stick-slip dynamics of granular materials can be seen as the jamming-unjamming process accompanied by the formation and buckling of force chains, which are triggered by localized particle rearrangements known as microslips or local avalanches (Barés et al., 2017; Gao et al., 2019).

The spatial distributions of microslips that occurred during the recharge and drop stage can be further quantified using the normalized spatial correlation function (see Text S2) (Ma et al.,

2019, 2021). We group the recharge and drop events according to the magnitude and sign of stress fluctuation. Logarithmic binning is used. Figure 2d shows the normalized correlation functions $C_{D^2_{min}}(r)$ for recharge and drop events of different magnitudes. The spatial autocorrelation decays rapidly within a short distance of several d_{50}, showing a short-range ordering. Solid lines indicate that the decay of correlations with r are reasonably well fitted by the Ornstein-Zernike function as $C_{D^2_{min}}(r) \propto r^{-0.5}\exp(-r/\xi_r)$. We can see that the correlation length of microslips ξ_r remains nearly unchanged for recharge events and increases rapidly for large stress drop (see red line and left axis of Figure 2e). This trend indicates that a more cooperative and concentrated distribution of microslips constitutes the microscopic origin of global slip avalanche.

The spatial autocorrelation of microslips can also be quantified by global Moran's *I* (see Text S2) (Ma et al., 2019, 2021). The Moran's *I* of particle $D^2_{\min}$ for recharge and drop events of different magnitudes show a very similar trend as the correlation length ξ_r (see blue line and right axis of Figure 2e). The spatial correlation analysis of microslips indicates that the spatially correlated microslips forming large shear transition zones are responsible for the stress drop and frictional weakening. The stress drop increases with the increasing degree of aggregation of microslips. The spatial distribution of microslips during recharge stages shows on average a plateau over different bins.

3.2 Machine learning predicts the stress fluctuations

In order to establish the quantitative relation between microslips and the magnitude of global stress fluctuation, we resort to use the Extreme Gradient Boosting (XGBoost) technique to interrogate the data (Chen & Guestrin, 2016). Different from the Deep Learning, we need to extract physically reasonable features from the raw data for input for the Machine Learning (ML). The above analysis demonstrates a clear difference of microslips between recharge and drop events. Therefore, it is necessary to consider both the statistical and spatial characteristics of microslips in the feature extraction. We first calculate the maximum, mean, variance, skewness, and kurtosis of particle $D^2_{\min}$ within each particle's second-neighbor shell (see Figure 3a), corresponding to the second minimum of pair correlation function shown in Figure S1a. These statistics contain information on how particle $D^2_{\min}$ distributes in space. We then calculate the statistical features of each particle's medium range statistics (see Figure 3b). The statistical operator includes mean, max, variance, percentiles, and various higher-order moments. These statistical features are connected as the medium-range feature vector (MRF).

To highlight the importance of the spatial pattern of microslips in the prediction of global stress fluctuation, we also calculate the statistical features of particles $D^2_{\min}$ as the input vector for XGBoost model training. This feature vector does not contain any information about the spatial distribution of microslips, and is referred to as particle-scale feature vector (PSF). MRF and PSF

are extracted for each recharge/drop event, and the corresponding output of XGBoost is the global stress fluctuation of the recharge/drop event. A typical structure of a XGBoost is depicted in Figure 3c. The XGBoost modeling process is briefly introduced in Text S3.

The shuffled dataset is divided into training set, test set, and validation set, with a proportion of 60%, 20%, and 20%, respectively. The three sets do not overlap each other to avoid "information leakage". The loss function of XGBoost for regression problems is the mean square error (MSE). The hyperparameters of XGBoost are tuned using Bayesian Optimization (Snoek et al., 2012). The performance of XGBoost models using PSF and MRF as inputs are shown in Figure 3d and Figure 3e, respectively. As can be seen, the trained XGBoost models not only classify the recharge and drop event from the microslips, but also predict the magnitude of stress fluctuation with good accuracy. By taking into account both statistical and spatial characteristics of the microslips, the trained XGBoost model exhibits better performance with a coefficient of determination $R^2 = 0.78$.

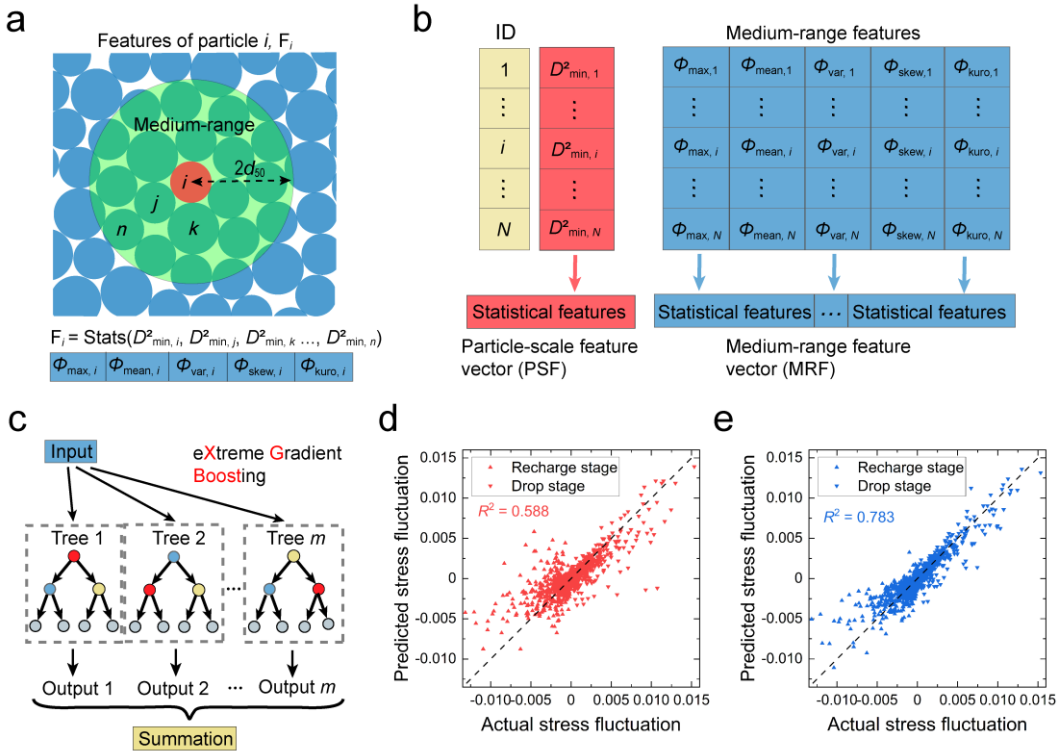

Figure 3. Machine learning builds the bridge between microslips and global stress fluctuation. (a) The statistical characteristics of particle $D^2_{\min}$ within each particle's second-neighbor shell. (b) Feature extraction process: particle-scale feature vector (red column) and medium-range feature vector (blue columns). These two feature vectors are fed as input to the downstream XGBoost model to predict global stress fluctuation. (c) Schematic of XGBoost (a supervised ML approach) based on the gradient boosting decision. Performance of XGBoost model trained by (d) PSF and (e) MRF, respectively.

Figure 3e depicts that certain success can be achieved in learning the complex relations between local and global avalanches for prediction. We further analyze the feature importance of the

XGBoost model trained by MRF. The feature importance is quantified by Shapley Additive Explanation (SHAP) value (Lundberg & Lee, 2017). The SHAP value for each feature is the average marginal contribution of a feature value across all possible coalitions, representing their contribution towards a higher or lower final prediction. Figure 4a shows the mean absolute SHAP values of the top 10 important features. The mean value of ϕ_{kurt} is the most important feature, changing the predicted absolute stress fluctuation on average by 0.6 percentage points.

ϕ_{kurt} measures the tail-heaviness of $D^2_{\min}$ of a particle's second nearest neighbors (Westfall, 2014). The smaller ϕ_{kurt} indicates the considered particle and its neighbors move in a corporative manner, i.e., particles with either high $D^2_{\min}$ or low $D^2_{\min}$ are spatially clustered. To investigate how the mean ϕ_{kurt} affects the model prediction, we present the SHAP dependence plot in Figure 4b. Each dot denotes a recharge/drop event in the ML dataset, and the scatters are colored according to the global Moran's I of particle $D^2_{\min}$. The higher mean ϕ_{kurt} results in smaller and negative SHAP value, pushing the XGBoost prediction towards a recharge event. In contrast, microslips of a drop event demonstrate stronger spatial correlation and thus have smaller ϕ_{kurt}. This feature helps XGBoost to distinguish between the recharge and drop events and predict the magnitude of global stress fluctuation. This study reveals that the spatial distribution of microslips contains key information on the stress state of a granular gouge such that microslips (e.g., local acoustic emission signal and local seismic wave) detected inside the natural gouge faults may also serve useful to predict its frictional stability.

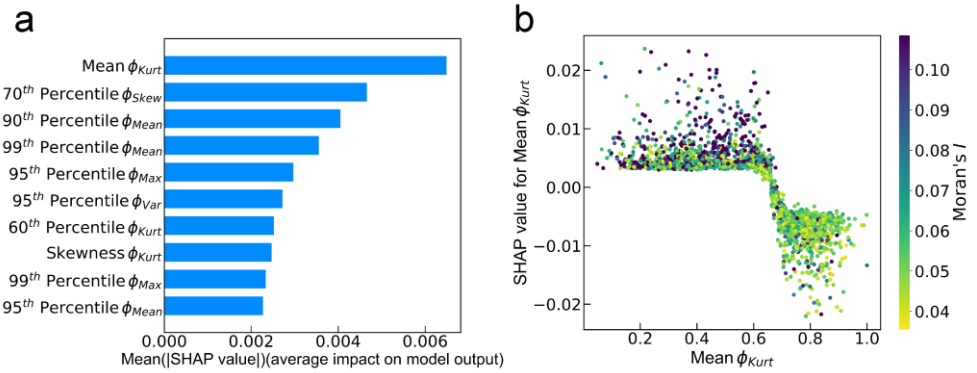

Figure 4. Feature importance analysis. (a) SHAP values for the top 10 important features. (b) Dependence plot for the mean value of ϕ_{kurt}, colored by the global moran's I.

4 Conclusions

We numerically investigated the relations between microslips and global stress fluctuation of a slowly sheared granular gouge. The microslip is manifested as irresible particle rearrangement and is quantified by nonaffine particle motion. The statistical features and spatial distributions of microslips that occurred during the rechage and drop stages of a stick-slip cycle demonstrate apprantely different characteristics. Both the Moran's I and the correlation length of particle $D^2_{\min}$ indicate that microslips in the drop stage are spatially correlated to form large local

avalanches, leading to large stress drop and frictional weakening. The difference in the microscopic dynamics of recharge and drop events suggest that we may quantitatively connect the microslips and global stress fluctuation.

The use of XGBoost boosts to build the bridge between microslips and macro stress fluctuation. Two sets of input fractures are extracted from the raw data to train the ML models. By using the input feature vector containing both statistical and spatial information of microslips, the trained XGBoost model can not only distinguish btween recharge and drop events but also predict the magnitude of stress fluctuation with good accurancy. The feature importance analysis by SHAP values reveals that the kurtosis of $D^2_{\min}$ within each particle's first and second nearest neighbors is the most important feature, which characterize the local spatial autocorrelation of microslips. We conclude that the spatial distributions of microslips contain key information about the stress state of granular gouge fault and its frictional stability. It should be noted that there are many other ways to extract the spatial patterns of microslips, such as Convolutional Neural Network, Graph Embedding for feature extraction, and complex network analysis. This study may shed lights into the mechanisms governing earthquake nucleation, microslips, friction fluctuations, and their connection during the stick-slip dynamics of earthquake cycles.

Acknowledgments, Samples, and Data

We acknowledge the financial support from the National Natural Science Foundation of China (Grant No. 51825905, U1865204, and 51779194) and Science project of China Huaneng Group Co. Ltd (HNKJ18-H26). The numerical calculations in this work have been done on the supercomputing system in the Supercomputing Center of Wuhan University. The data supporting this paper can all be found at the corresponding author's figshare repository (https://figshare.com/articles/dataset/Machine_learning_bridges_microslips_and_slip_avalanches_of_sheared_granular_gouge/14099417).

References

Aharonov, E., & Sparks, D. (2004). Stick-slip motion in simulated granular layers. *Journal of Geophysical Research: Solid Earth*, *109*(9), 1–12. https://doi.org/10.1029/2003JB002597

Barés, J., Wang, D., Wang, D., Bertrand, T., O'Hern, C. S., & Behringer, R. P. (2017). Local and global avalanches in a two-dimensional sheared granular medium. *Physical Review E*, *96*(5), 1–13. https://doi.org/10.1103/PhysRevE.96.052902

Baró, J., Corral, Á., Illa, X., Planes, A., Salje, E. K. H., Schranz, W., et al. (2013). Statistical similarity between the compression of a porous material and earthquakes. *Physical Review Letters*, *110*(8), 1–5. https://doi.org/10.1103/PhysRevLett.110.088702

Bergen, K. J., Johnson, P. A., De Hoop, M. V., & Beroza, G. C. (2019). Machine learning for data-driven discovery in solid Earth geoscience. *Science*, *363*(6433). https://doi.org/10.1126/science.aau0323

Bolton, D. C., Marone, C., Shokouhi, P., Rivière, J., Rouet-Leduc, B., Hulbert, C., & Johnson, P. A. (2019). Characterizing acoustic signals and searching for precursors during the laboratory seismic cycle using unsupervised machine learning. *Seismological Research Letters*. https://doi.org/10.1785/0220180367

Bolton, D. C., Shreedharan, S., Rivière, J., & Marone, C. (2020). Acoustic Energy Release During the Laboratory Seismic Cycle: Insights on Laboratory Earthquake Precursors and Prediction. *Journal of Geophysical Research: Solid Earth*, *125*(8). https://doi.org/10.1029/2019JB018975

Byerlee, J. D., & Brace, W. F. (1966). Stick-Slip as a Mechanism for Earthquakes. *Science*, *153*(3739), 990–992.

Cao, P., Dahmen, K. A., Kushima, A., Wright, W. J., Park, H. S., Short, M. P., & Yip, S. (2018). Nanomechanics of

slip avalanches in amorphous plasticity. *Journal of the Mechanics and Physics of Solids*, *114*, 158–171. https://doi.org/10.1016/j.jmps.2018.02.012

Cao, P., Short, M. P., & Yip, S. (2019). Potential energy landscape activations governing plastic flows in glass rheology. *Proceedings of the National Academy of Sciences of the United States of America*, *116*(38), 18790–18797. https://doi.org/10.1073/pnas.1907317116

Castellanos, D. F., & Zaiser, M. (2018). Avalanche Behavior in Creep Failure of Disordered Materials. *Physical Review Letters*, *121*(12), 125501. https://doi.org/10.1103/PhysRevLett.121.125501

Cipelletti, L., Martens, K., & Ramos, L. (2019). Microscopic precursors of failure in soft matter. *Soft Matter*, *16*(1), 82–93. https://doi.org/10.1039/c9sm01730e

Corbi, F., Sandri, L., Bedford, J., Funiciello, F., Brizzi, S., Rosenau, M., & Lallemand, S. (2019). Machine Learning Can Predict the Timing and Size of Analog Earthquakes. *Geophysical Research Letters*, *46*(3), 1303–1311. https://doi.org/10.1029/2018GL081251

Denisov, D. V., Lörincz, K. A., Uhl, J. T., Dahmen, K. A., & Schall, P. (2016). Universality of slip avalanches in flowing granular matter. *Nature Communications*, *7*. https://doi.org/10.1038/ncomms10641

Dorostkar, O., & Carmeliet, J. (2018). Potential Energy as Metric for Understanding Stick–Slip Dynamics in Sheared Granular Fault Gouge: A Coupled CFD–DEM Study. *Rock Mechanics and Rock Engineering*, *51*(10), 3281–3294. https://doi.org/10.1007/s00603-018-1457-6

Dorostkar, O., & Carmeliet, J. (2019). Grain Friction Controls Characteristics of Seismic Cycle in Faults With Granular Gouge. *Journal of Geophysical Research: Solid Earth*, *124*(7), 6475–6489. https://doi.org/10.1029/2019JB017374

Dorostkar, O., Guyer, R. A., Johnson, P. A., Marone, C., & Carmeliet, J. (2017a). On the micromechanics of slip events in sheared, fluid-saturated fault gouge. *Geophysical Research Letters*, *44*(12), 6101–6108. https://doi.org/10.1002/2017GL073768

Dorostkar, O., Guyer, R. A., Johnson, P. A., Marone, C., & Carmeliet, J. (2017b). On the role of fluids in stick-slip dynamics of saturated granular fault gouge using a coupled computational fluid dynamics-discrete element approach. *Journal of Geophysical Research: Solid Earth*, *122*(5), 3689–3700. https://doi.org/10.1002/2017JB014099

Dorostkar, O., Guyer, R. A., Johnson, P. A., Marone, C., & Carmeliet, J. (2018). Cohesion-Induced Stabilization in Stick-Slip Dynamics of Weakly Wet, Sheared Granular Fault Gouge. *Journal of Geophysical Research: Solid Earth*, *123*(3), 2115–2126. https://doi.org/10.1002/2017JB015171

Ferdowsi, B., Griffa, M., Guyer, R. A., Johnson, P. A., Marone, C., & Carmeliet, J. (2013). Microslips as precursors of large slip events in the stick-slip dynamics of sheared granular layers: A discrete element model analysis. *Geophysical Research Letters*, *40*(16), 4194–4198. https://doi.org/10.1002/grl.50813

Ferdowsi, B., Griffa, M., Guyer, R. A., Johnson, P. A., & Carmeliet, J. (2014a). Effect of boundary vibration on the frictional behavior of a dense sheared granular layer. *Acta Mechanica*, *225*(8), 2227–2237. https://doi.org/10.1007/s00707-014-1136-y

Ferdowsi, B., Griffa, M., Guyer, R. A., Johnson, P. A., Marone, C., & Carmeliet, J. (2014b). Three-dimensional discrete element modeling of triggered slip in sheared granular media. *Physical Review E - Statistical, Nonlinear, and Soft Matter Physics*, *89*(4), 1–12. https://doi.org/10.1103/PhysRevE.89.042204

Ferdowsi, B., Griffa, M., Guyer, R. A., Johnson, P. A., Marone, C., & Carmeliet, J. (2015). Acoustically induced slip in sheared granular layers: Application to dynamic earthquake triggering. *Geophysical Research Letters*, *42*(22), 9750–9757. https://doi.org/10.1002/2015GL066096

Gao, K., Euser, B. J., Rougier, E., Guyer, R. A., Lei, Z., Knight, E. E., et al. (2018). Modeling of Stick-Slip Behavior in Sheared Granular Fault Gouge Using the Combined Finite-Discrete Element Method. *Journal of Geophysical Research: Solid Earth*. https://doi.org/10.1029/2018JB015668

Gao, K., Guyer, R., Rougier, E., Ren, C. X., & Johnson, P. A. (2019). From Stress Chains to Acoustic Emission. *Physical Review Letters*, *123*(4). https://doi.org/10.1103/PhysRevLett.123.048003

Hulbert, C., Rouet-Leduc, B., Johnson, P. A., Ren, C. X., Rivière, J., Bolton, D. C., & Marone, C. (2019). Similarity of fast and slow earthquakes illuminated by machine learning. *Nature Geoscience*, *12*(1), 69–74. https://doi.org/10.1038/s41561-018-0272-8

Johnson, P. A., Ferdowsi, B., Kaproth, B. M., Scuderi, M., Griffa, M., Carmeliet, J., et al. (2013). Acoustic emission and microslip precursors to stick-slip failure in sheared granular material. *Geophysical Research Letters*, *40*(21), 5627–5631. https://doi.org/10.1002/2013GL057848

Kloss, C., Goniva, C., Hager, A., Amberger, S., & Pirker, S. (2012). Models , algorithms and validation for opensource DEM and CFD-DEM. *Progress in Computational Fluid Dynamics*, *12*(2–3), 140–152.

Leeman, J. R., Saffer, D. M., Scuderi, M. M., & Marone, C. (2016). Laboratory observations of slow earthquakes

and the spectrum of tectonic fault slip modes. *Nature Communications*, *7*, 1–6. https://doi.org/10.1038/ncomms11104

Liu, J., Wautier, A., Bonelli, S., Nicot, F., & Darve, F. (2020). Macroscopic softening in granular materials from a mesoscale perspective. *International Journal of Solids and Structures*, *193–194*, 222–238. https://doi.org/10.1016/j.ijsolstr.2020.02.022

Lundberg, S. M., & Lee, S. I. (2017). A unified approach to interpreting model predictions. *Advances in Neural Information Processing Systems 30*, 4765–4774.

Ma, G., Regueiro, R. A., Zhou, W., Wang, Q., & Liu, J. (2018). Role of particle crushing on particle kinematics and shear banding in granular materials. *Acta Geotechnica*, *13*(3), 601–618. https://doi.org/10.1007/s11440-017-0621-6

Ma, G., Regueiro, R. A., Zhou, W., & Liu, J. (2019). Spatiotemporal analysis of strain localization in dense granular materials. *Acta Geotechnica*, *14*(4), 973–990. https://doi.org/10.1007/s11440-018-0685-y

Ma, G., Zou, Y., Gao, K., Zhao, J., & Zhou, W. (2020). Size Polydispersity Tunes Slip Avalanches of Granular Gouge. *Geophysical Research Letters*, *47*(23), 1–9. https://doi.org/10.1029/2020gl090458

Ma, G., Zou, Y., Chen, Y., Tang, L., Ng, T. tat, & Zhou, W. (2021). Spatial correlation and temporal evolution of plastic heterogeneity in sheared granular materials. *Powder Technology*. https://doi.org/10.1016/j.powtec.2020.09.053

Mair, K., & Hazzard, J. F. (2007). Nature of stress accommodation in sheared granular material: Insights from 3D numerical modeling. *Earth and Planetary Science Letters*, *259*(3–4), 469–485. https://doi.org/10.1016/j.epsl.2007.05.006

Mair, K., Frye, K. M., & Marone, C. (2002). Influence of grain characteristics on the friction of granular shear zones. *Journal of Geophysical Research: Solid Earth*, *107*(B10), ECV 4-1-ECV 4-9. https://doi.org/10.1029/2001jb000516

Marone, C. (1998). The effect of loading rate on static friction and the rate of fault healing during the earthquake cycle. *Nature*, *391*(6662), 69–72. https://doi.org/10.1038/34157

Marone, C. (2018). Training machines in Earthly ways. *Nature Geoscience*, *11*(5), 301–302. https://doi.org/10.1038/s41561-018-0117-5

Marone, C., Scholtz, C. H., & Bilham, R. (1991). On the mechanics of earthquake afterslip. *Journal of Geophysical Research*, *96*(B5), 8441–8452. https://doi.org/10.1029/91JB00275

Mousavi, S. M., & Beroza, G. C. (2020). A Machine-Learning Approach for Earthquake Magnitude Estimation. *Geophysical Research Letters*, *47*(1), 1–7. https://doi.org/10.1029/2019GL085976

Mousavi, S. M., Ellsworth, W. L., Zhu, W., Chuang, L. Y., & Beroza, G. C. (2020). Earthquake transformer—an attentive deep-learning model for simultaneous earthquake detection and phase picking. *Nature Communications*, *11*(1), 1–12. https://doi.org/10.1038/s41467-020-17591-w

Nanjo, K. Z. (2020). Were changes in stress state responsible for the 2019 Ridgecrest, California, earthquakes? *Nature Communications*, *11*(1), 3–6. https://doi.org/10.1038/s41467-020-16867-5

Niemeijer, A., Marone, C., & Elsworth, D. (2010). Frictional strength and strain weakening in simulated fault gouge: Competition between geometrical weakening and chemical strengthening. *Journal of Geophysical Research: Solid Earth*, *115*(10), 1–16. https://doi.org/10.1029/2009JB000838

Rathbun, A. P., Renard, F., & Abe, S. (2013). Numerical investigation of the interplay between wall geometry and friction in granular fault gouge. *Journal of Geophysical Research: Solid Earth*, *118*(3), 878–896. https://doi.org/10.1002/jgrb.50106

Ren, C. X., Dorostkar, O., Rouet-Leduc, B., Hulbert, C., Strebel, D., Guyer, R. A., et al. (2019). Machine Learning Reveals the State of Intermittent Frictional Dynamics in a Sheared Granular Fault. *Geophysical Research Letters*, *46*(13), 7395–7403. https://doi.org/10.1029/2019GL082706

Ren, C. X., Hulbert, C., Johnson, P. A., & Rouet-Leduc, B. (2020). Machine learning and fault rupture: A review. *Advances in Geophysics*, *61*, 57–107. https://doi.org/10.1016/bs.agph.2020.08.003

Rivière, J., Lv, Z., Johnson, P. A., & Marone, C. (2018). Evolution of b-value during the seismic cycle: Insights from laboratory experiments on simulated faults. *Earth and Planetary Science Letters*, *482*, 407–413. https://doi.org/10.1016/j.epsl.2017.11.036

Rouet-Leduc, B., Hulbert, C., Lubbers, N., Barros, K., Humphreys, C. J., & Johnson, P. A. (2017). Machine Learning Predicts Laboratory Earthquakes. *Geophysical Research Letters*, *44*(18), 9276–9282. https://doi.org/10.1002/2017GL074677

Rouet-Leduc, B., Hulbert, C., Bolton, D. C., Ren, C. X., Riviere, J., Marone, C., et al. (2018). Estimating Fault Friction From Seismic Signals in the Laboratory. *Geophysical Research Letters*, *45*(3), 1321–1329. https://doi.org/10.1002/2017GL076708

Rouet-Leduc, B., Hulbert, C., & Johnson, P. A. (2019). Continuous chatter of the Cascadia subduction zone revealed by machine learning. *Nature Geoscience*, *12*(1), 75–79. https://doi.org/10.1038/s41561-018-0274-6

Scuderi, M. M., Carpenter, B. M., Johnson, P. A., & Marone, C. (2015). Poromechanics of stick-slip frictional sliding and strength recovery on tectonic faults. *Journal of Geophysical Research: Solid Earth*, *120*(10), 6895–6912. https://doi.org/10.1002/2015JB011983.

Scuderi, M. M., Marone, C., Tinti, E., Di Stefano, G., & Collettini, C. (2016). Precursory changes in seismic velocity for the spectrum of earthquake failure modes. *Nature Geoscience*, *9*(9), 695–700. https://doi.org/10.1038/ngeo2775

Snoek, J., Larochelle, H., & Adams, R. P. (2012). Practical Bayesian Optimization of Machine Learning Algorithms. *Proceedings of the 25th International Conference on Neural Information Processing Systems*, *25*, 2951–2959.

Song, D., Ng, C. W. W., Choi, C. E., Zhou, G. G. D., Kwan, J. S. H., & Koo, R. C. H. (2017). Influence of debris flow solid fraction on rigid barrier impact. *Canadian Geotechnical Journal*, *54*(10), 1421–1434. https://doi.org/10.1139/cgj-2016-0502

Sun, B. A., Pauly, S., Tan, J., Stoica, M., Wang, W. H., Kühn, U., & Eckert, J. (2012). Serrated flow and stick-slip deformation dynamics in the presence of shear-band interactions for a Zr-based metallic glass. *Acta Materialia*, *60*(10), 4160–4171. https://doi.org/10.1016/j.actamat.2012.04.013

Chen, T., & Guestrin, C. (2016). XGBoost: A Scalable Tree Boosting System. *The Journal of the Association of Physicians of India*, *42*(8), 665.

Tinti, E., Scuderi, M. M., Scognamiglio, L., Di Stefano, G., Marone, C., & Collettini, C. (2016). On the evolution of elastic properties during laboratory stick-slip experiments spanning the transition from slow slip to dynamic rupture. *Journal of Geophysical Research: Solid Earth*, *121*(12), 8569–8594. https://doi.org/10.1002/2016JB013545

Trugman, D. T., Mcbrearty, I. W., Bolton, D. C., Robert, A., Marone, C., & Johnson, P. A. (2020). The Spatio-temporal Evolution of Granular Microslip Precursors to Laboratory Earthquakes. *Geophysical Research Letters*, 1–10. https://doi.org/10.1029/2020GL088404

Wang, D., Carmeliet, J., Zhou, W., & Dorostkar, O. (2020). On the effect of grain fragmentation on frictional instabilities in faults with granular gouge. EarthArxiv.

Westfall, P. H. (2014). Kurtosis as Peakedness, 1905–2014. R.I.P. *American Statistician*, *68*(3), 191–195. https://doi.org/10.1080/00031305.2014.917055

Zheng, J., Sun, A., Wang, Y., & Zhang, J. (2018). Energy Fluctuations in Slowly Sheared Granular Materials. *Physical Review Letters*, *121*(24), 248001. https://doi.org/10.1103/PhysRevLett.121.248001